Journal of Agricultural Science and Technology (JAST), 28(4)
In Press, Pre-Proof Version

Mapping Agricultural Drought Hazard in Iran

Abdolraoof Shahozei[1], Peyman Mahmoudi[1*], and Seyed Mahdi Amir Jahanshahi[2]

ABSTRACT

The primary objective of this study is to develop a spatially explicit Agricultural Drought Hazard (ADH) map for Iran by integrating precipitation and soil moisture data. For this, two key datasets spanning 30 years (1987-2016) were utilized: monthly precipitation from 63 synoptic stations (Iran's Meteorological Organization) and gridded (0.5°x0.5°) monthly soil moisture from the Climate Prediction Center (CPC). These were transformed into the Standardized Precipitation Index (SPI) and Standardized Soil Moisture Index (SSMI), respectively. A core quantitative finding is the regionally distinct correlation between SPI and SSMI: the strongest positive correlations were observed in Iran's expansive dry climates (southern and eastern halves), while significantly weaker correlations characterized the more humid northern and western halves. This indicates a more rapid and direct propagation of meteorological drought to agricultural drought in arid zones. These standardized indices were then integrated to construct Iran's ADH map. This map quantitatively classifies the central, southern, and southeastern regions as experiencing 'high' and 'very high' agricultural drought hazard. These findings provide a critical, data-driven tool for national and regional policymakers, offering improved insights for targeted drought mitigation and water resource management compared to single-indicator assessments, particularly crucial for Iran's vulnerable agricultural sector.

Author keywords: Drought, Hazard, Iran, Precipitation, Soil moisture.

Introduction

Drought, characterized by a significant shortage of precipitation over a period (Wilhite, 2005), stands as one of the most complex and impactful climatic hazards globally (Ghorbani et al., 2019). Its insidious onset and prolonged duration often result in severe and cascading economic, social, and environmental consequences (Kao et al., 2021; Erfurt et al., 2019), particularly threatening water resource availability and agricultural productivity, which forms the backbone of many economies, especially in arid and semi-arid regions.

[1] Department of Physical Geography, Faculty of Geography and Environmental Planning, University of Sistan and Baluchestan, Zahedan, Islamic Republic of ran.
[2] Department of Statistics, Faculty of Mathematics, Statistics and Computer Science, University of Sistan and Baluchestan, Zahedan, Iran
*Corresponding author; e-mail: p_mahmoudi@gep.usb.ac.ir

Effective drought monitoring and management necessitate its quantification, leading to the development of numerous indices over recent decades. These indices typically categorize droughts based on their primary impact: meteorological (precipitation deficits), agricultural (soil moisture shortages impacting crop yields and thereby food security), and hydrological (reduced surface and groundwater) (Chanda et al., 2014). Within meteorological drought assessment, the Standardized Precipitation Index (SPI) (McKee et al., 1993) and the Standardized Precipitation Evapotranspiration Index (SPEI) (Vicente-Serrano et al., 2010) are widely adopted. Their strength lies in standardizing deviations in precipitation (SPI) or climatic water balance (SPEI), allowing for versatile multi-scalar analysis and cross-regional comparisons. For agricultural drought, which directly impacts rural livelihoods and regional economies, indices like the Standardized Soil Moisture Index (SSMI) (e.g., Modarres, 2007; Kao & Govindaraj, 2010) quantify deficits in soil moisture, often employing a standardization approach akin to SPI. While these category-specific indices are invaluable for characterizing particular drought facets, relying solely on individual metrics can obscure the multifaceted nature of drought and its cascading impacts, particularly when assessing comprehensive drought risk.

The inherent complexity and multi-dimensional impacts of drought underscore the limitations of relying on single, univariate indices for a comprehensive assessment of its detrimental effects. Consequently, contemporary drought management increasingly adopts a 'risk'-based framework. This framework posits that risk arises not solely from the natural hazard itself (e.g., meteorological drought intensity), but from the intricate interplay between the drought hazard (characterized by its frequency, severity, and duration) and the vulnerability of exposed systems (e.g., agriculture, water resources, socio-economic structures) (Shahid and Behrawan, 2008; Nasrollahi et al., 2018; Hagenlocher et al., 2019). Within this paradigm, quantifying the drought hazard component is a critical first step, typically achieved by analyzing patterns and characteristics derived from various drought indices (Blauhut et al., 2015). However, translating information from one or more drought indices into spatially explicit and practically applicable drought hazard maps—which are crucial for informing overall risk assessments and guiding proactive mitigation strategies—presents ongoing methodological considerations and has been approached in diverse ways in existing literature.

Building on this, the literature reveals several approaches to constructing drought hazard maps, often as a crucial input for broader risk assessments. One prevalent strategy, exemplified by Shahid and Behrawan (2008) in their study of western Bangladesh, involves a multi-stage

process focused on deriving a drought hazard map using the Standardized Precipitation Index (SPI). Their methodology included: (i) extracting the frequency of different SPI-defined drought severity classes for study stations, (ii) calculating the probability of occurrence for each class, and (iii) assigning impact-based weights (ranging from 1 for weak to 4 for extreme drought). The final hazard map was then generated by aggregating the product of these weights and occurrence probabilities. Variations of this weighted, frequency-based approach to hazard mapping, primarily utilizing indices like SPI, have been similarly applied in other regional contexts such as Indonesia (Avia et al., 2023), Iran (Nasrollahi et al., 2018), and South Korea (Kim et al., 2015), highlighting its utility in transforming index data into spatially explicit hazard assessments.

While frequency analysis of meteorological indices like SPI, as discussed previously, offers one pathway to hazard mapping, other research has focused on agricultural drought and incorporated diverse data sources. Faridatul and Ahmed (2020), for example, employed the satellite-derived Modified Vegetation Condition Index (mVCI) to map agricultural drought hazard across Bangladesh, assigning coefficients based on severity classes. The integration of vegetation health into hazard assessment is also seen in the work of Yu et al. (2018), who combined SPI with the Vegetation Condition Index (VCI) for drought hazard mapping in north of South Korea, contrasting with approaches like Daneshvar et al. (2012) in Iran which relied primarily on SPI. Further illustrating methodological diversity, Adnan and Ullah (2020) developed an empirical model for Pakistan that integrated the frequency of various drought classes with seasonal soil moisture characteristics to derive a multi-level drought hazard map. These examples collectively illustrate the ongoing exploration of different indices, data integration techniques, and classification schemes in the pursuit of robust drought hazard characterization.

The preceding review highlights a spectrum of methodologies for drought hazard assessment. However, for a country like Iran, characterized by its arid to semi-arid climate, significant water scarcity, and high dependence on climate-sensitive agriculture (Vaghefi et al., 2019; Mahmoudi et al., 2019b), the translation of hazard information into comprehensive, national-scale drought risk assessments remains a critical imperative. Recent climatic variabilities and severe drought episodes have already imposed substantial economic burdens, underscoring the urgent need for robust planning tools. While existing approaches, such as the empirical model by Adnan and Ullah (2020) for drought hazard mapping, offer valuable foundations, a clear gap exists in adapting and enhancing such techniques to develop integrated drought risk maps

that also consider underlying vulnerabilities at a national scale for Iran. This study aims to address this gap. Therefore, the primary objective of this research is to develop a national drought risk map for Iran by refining and advancing the empirical modeling approach previously utilized for hazard assessment by Adnan and Ullah (2020), specifically by incorporating a tailored assessment of Iran's diverse precipitation regimes and their associated vulnerabilities through a novel, country-specific classification and weighting scheme integrated into the ADHI (Agricultural Drought Hazard Index) framework. The anticipated contributions of this work are threefold: (1) to present an enhanced methodological framework for national-scale drought risk assessment tailored to arid/semi-arid regions; (2) to deliver the first comprehensive, spatially explicit drought risk map for Iran using this improved methodology; and (3) to provide actionable insights for targeted drought mitigation, water resource management, and agricultural policy formulation in the country.

The study area

Iran is situated in the arid belt on the world map and a large part of its climate (over 90%) is arid. This land borders the water regions of the Caspian Sea in the north and the Persian Gulf and the Sea of Oman in the south. The spatial precipitation distribution in a large swathe of Iran is highly dependent on rough areas. Alborz mountains, which extend from western and eastern directions to the north, and Zagros mountains, which extend from northwestern to southeastern directions, control the entry of precipitating systems towards the central plateau. Surrounded by water areas and a large area of mountains, Iran enjoys a diverse climate (Figure 1a). According to the De Martonne classification index (De Martonne 1909), Iran's climate is generally arid (around 65%), semi-arid (around 20%), while only 10% of which is humid (Katiraie-Boroujerdy et al. 2013). The average annual precipitation in Iran is close to 250 mm, whose spatial distribution is highly different in various areas, with desert regions recording less than 250 mm and other areas such as the western boundaries of the Caspian Sea recording 1800 mm (Figure 1b) (Mahmoudi et al. 2021). The spatial distribution of the average annual precipitation of Iran is a function of rough areas and the changing angles of the sun's inclination. The lowest average annual temperature in Iran is noted in the northwest and the highest in the southeast coasts. In sum, the country's temperature sees a reduction from the south to the north and from the east to the west (Figure 1c) (Mahmoudi et al. 2021).

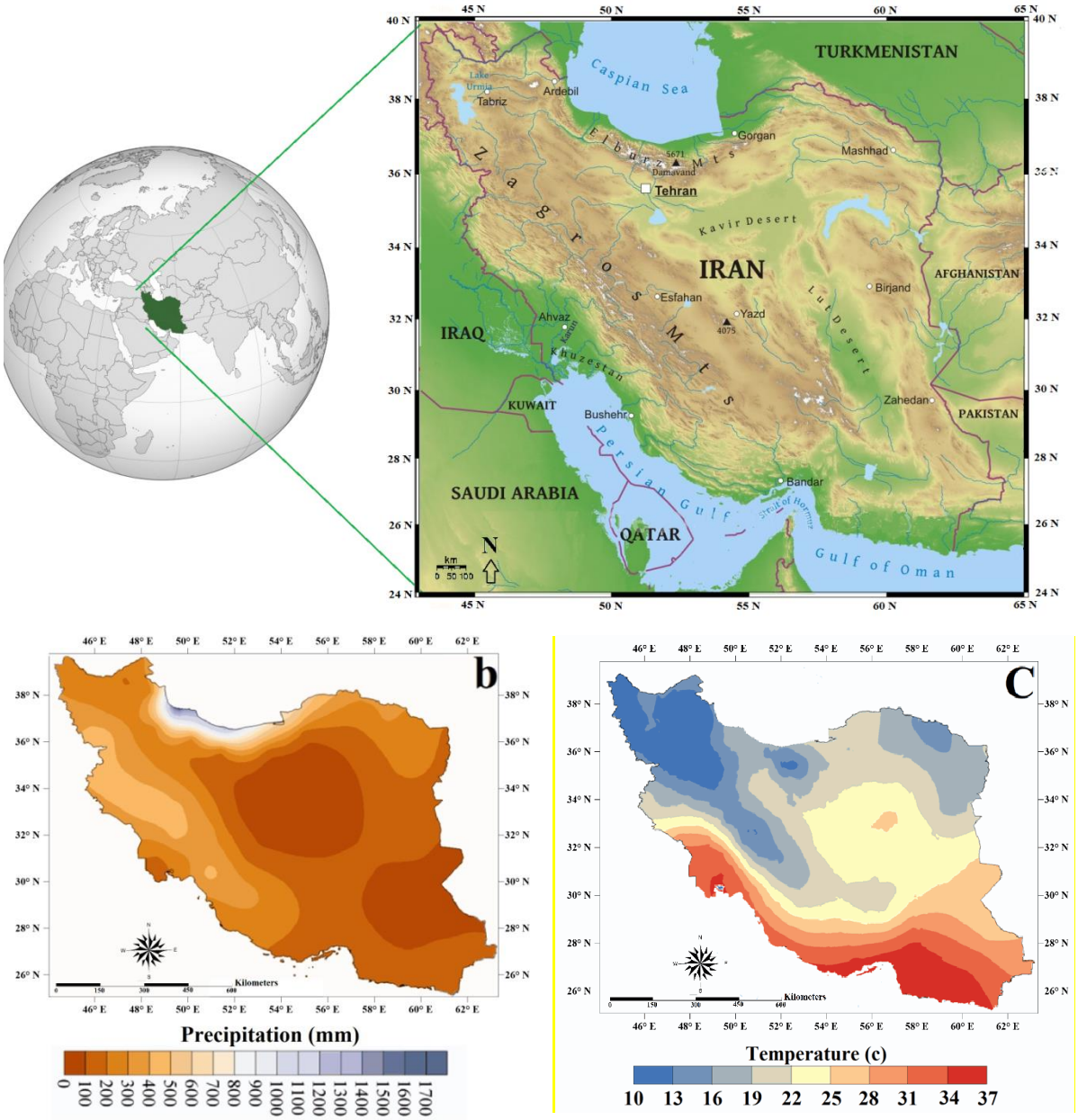

Figure 1. (a) Location and physical geography of Iran (Southwest Asia), (b) spatial distribution map of the mean annual precipitation (Mahmoudi et al. 2021), and (c) spatial distribution map of the mean annual temperature (Mahmoudi et al. 2021).

Data and Methods

Data

Two various databases are needed to prepare Iran's agricultural drought hazards map. The first database, comprising monthly precipitation data from 62 synoptic stations for 30 years (from 1987 to 2016), was received from Iran's Meteorological Organization. These stations were selected based on an adequate span of the statistical period (at least 30 years) and their spatial scattering across the country. The data were complete and reliable, with few missing values

reconstructed using correlation and linear regression methods (Asakereh, 2011). Figure 2 illustrates the distribution and scattering of the studied stations. To assign a representative area of influence to each station for the spatial representation of drought hazard, Thiessen's Polygon Method (Thiessen, 1911) was employed. We acknowledge the inherent limitations of this method in representing fine-scale spatial variability across Iran's diverse topography and microclimates, particularly its assumption of uniform conditions within polygons. However, it was utilized in this national-scale study because the primary Agricultural Drought Hazard Index (ADHI) calculations, which form the basis of the agricultural drought hazard map, were performed using the specific long-term precipitation records of each individual station. The Thiessen polygons then served as a standard approach to provide a first-order approximation for spatializing these station-based ADHI assessments and attributing the calculated hazard levels to distinct geographical areas across the country. Consequently, the calculations and analyses for the agricultural drought hazard map were developed based on these station-specific ADHI values and then regionalized using the areas defined by the Thiessen polygons (Figure 2)

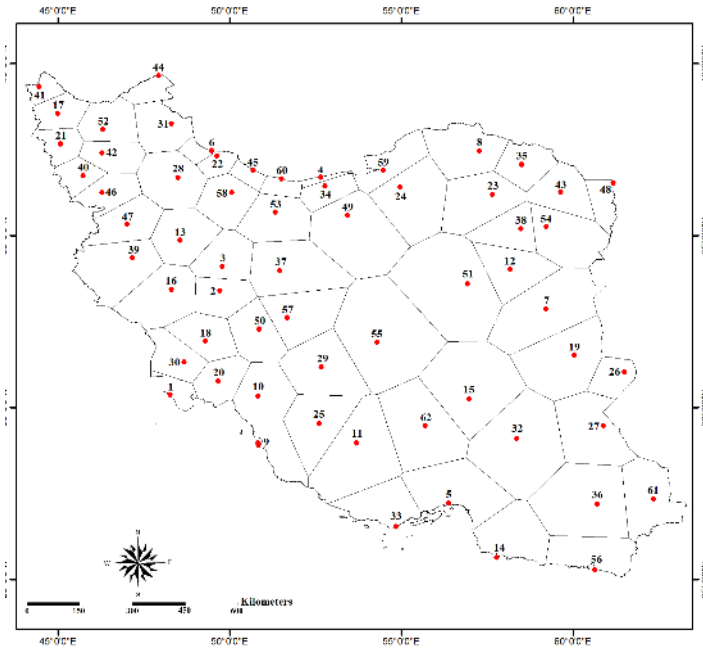

Station name	Code	Station name	Code	Station name	Code
Abadan	1	Rasht	22	Mashhad	43
Aligudarz	2	Sabzevar	23	Parsabad	44
Arak	3	Shahrud	24	Ramsar	45
Babolsar	4	Shiraz	25	Saqez	46
Bandarabbas	5	Zabol	26	Sanandaj	47
Bandar Anzali	6	Zahedan	27	Sarakhs	48
Birjand	7	Zanjan	28	Semnan	49
Bojnurd	8	Abadeh	29	Shahrekord	50
Bushehr	9	Ahvaz	30	Tabas	51
Dogonbadan	10	Ardabil	31	Tabriz	52
Fasa	11	Bam	32	Tehran	53
Ferdows	12	B. Lengeh	33	T. Heydariyeh	54
Hamedan	13	Gharakhil	34	Yazd	55
Jask	14	Quchan	35	Chabahar	56
Kerman	15	Iranshahr	36	Esfahan	57
Khorramabad	16	Kashan	37	Qazvin	58
Khoy	17	Kashmar	38	Gorgan	59
M. Soleyman	18	Kermanshah	39	Nowshahr	60
Nehbandan	19	Mahabad	40	Saravan	61
Omidiyeh	20	Maku	41	Sirjan	62
Orumiyeh	21	Maraghch	42		

Figure 2. Scattering and geographical situation of studied stations and the areas assigned to each station using Thiessen's Polygon Method.

The second database pertained to the gridded monthly amounts of soil moisture (0.5*0.5°, in millimeters per 1 meter of soil depth), downloaded from the Climate Prediction Center (CPC) (NOAA) (http://www.esrl.noaa.gov/psd/data/gridded/data.cpcsoil.htm) (Fan and van den Dool 2004), for the same 30-year time interval from 1987 to 2016. These data were not re-analysis

data, and it was argued that the re-analysis data could not be reliable due to their biases (van den Dool et al. 2003; Fan and van den Dool 2004). In sum, the number of gridded points extracted from the CPC (NOAA) database for the framework of Iran's political borders amounted to 622 gridded points. The time series of these data were complete and lacked any missing data. These data were validated by Mahmoudi et al. (2021) using soil moisture data measured at Iran's agricultural meteorological stations. Validation results suggested that the correlation coefficient between the gridded data of soil moisture and the stations located in arid and semi-arid regions in Iran was lower than 0.65, while the correlation coefficient between the gridded data of soil moisture and the stations located in humid regions was higher than 0.89.

Methods

Standardized Precipitation Index (SPI) and Standardized Soil Moisture Index (SSMI)

The Standardized Precipitation Index (SPI) is a tool originally developed by McKee et al. (1993; 1995) to identify and monitor droughts and their severity across various timescales. In the present study, all drought indices—including both the SPI and the Standardized Soil Moisture Index (SSMI)—were calculated and analyzed exclusively on an annual timescale. That is, the calculation steps for the SPI involved: (1) summing cumulative precipitation for each year using an annual timescale, (2) fitting gamma distribution functions to each hydrological year, (3) estimating distribution function values for total annual precipitation, and (4) converting the gamma-distributed values to standard normal variates. Since the SPI is essentially a z-score, it expresses the deviation of precipitation from the mean in units of standard deviation, facilitating comparison among sites and periods. Periods when the SPI is persistently negative, especially at -1 or lower, are regarded as drought events, which conclude when SPI values return to positive. Because all indices in this study were calculated over annual periods, all drought events and severity classifications are also defined on this annual basis (Table 1). Similarly, the Standardized Soil Moisture Index (SSMI), like the SPI, was calculated on an annual timescale (Gautam et al. 2023; Das et al. 2020; Lin et al. 2015), with drought severity determined using the thresholds summarized in Table 1.

188 **Table 1.** Classification of droughts based on the SPI and SSMI.

SPI value	Category
2.00 or more	Extreme wet
1.50 to 1.99	Severe wet
1.00 to 1.49	Moderate wet
0.50 to 0.99	Mild wet
0.49 to -0.49	Normal
-0.50 to -0.99	Mild drought
-1.00 to -1.49	Moderate drought
-1.50 to -1.99	Severe drought
-2.00 and less	Extreme drought

189 Reference: McKee et al. (1993).

190 **Agro-Climatic Regionalization using Moisture Index (MI)**

191 To provide a spatial context for the drought analysis across Iran's varied climatic conditions
192 and to enable a stratified assessment of drought characteristics, an agro-climatic regionalization
193 was undertaken using the Moisture Index (MI). The MI offers a quantitative measure of long-
194 term moisture availability by comparing mean annual precipitation (P) with mean annual
195 potential evapotranspiration (ETo) (Adnan et al., 2017).
196 For this study, the MI was calculated for the synoptic stations across the study area using long-
197 term (1986-2018) mean annual precipitation (P) data and corresponding mean annual potential
198 evapotranspiration (ETo) data, with ETo estimated using the FAO-56 Penman-Monteith
199 method. The MI was computed as a percentage according to Equation 1:

$$MI(\%) = \left[\frac{(P - ET_o)}{ET_o}\right] \times 100 \quad (1)$$

200
201 Subsequently, Iran was classified into distinct agro-climatic zones based on these MI values.
202 The classification framework initially proposed by Adnan et al. (2017), which outlines nine
203 classes, was adopted. For its application to Iran, this framework was refined by consolidating
204 certain adjacent classes: the "wet semi-arid" and "dry semi-arid" classes were merged into a
205 single "Semi-arid" category, and similarly, the "wet sub-humid" and "dry sub-humid" classes
206 were combined into a "Sub-humid" category. The MI thresholds for the original and the
207 reclassified categories adapted for Iran are detailed in Table 2.
208
209
210
211
212
213

Table 2. Agro-climatic classes of moisture index (MI) and its reclassification for Iran.

Agro-climatic classes	Symbol	MI limits (%)	Reclassification of the Agro-climatic classes	MI limits (%)
Extremely arid	A_e	<−90.0	Extremely arid	<−90.0
Arid	A	−90.0 to −80.0	Arid	−90.0 to −80.0
Dry semi-arid	SA_d	−79.9 to −56	semi-arid	−79.9 to −26.0
Wet semi-arid	SA_w	−55.9 to −26.0		
Dry sub-humid	SH_d	−25.9 to 0.0	sub-humid	−25.9 to –20.0
Wet sub-humid	SH_w	0.1 to –20.0		
Humid	H	20.1 to 50.0	Humid	20.1 to 50.0
Very humid	H_v	>50	Very humid	>50

To delineate the spatial distribution of these agro-climatic zones across Iran, the station-specific MI values were spatially interpolated using the Kriging method. The resulting map (Figure 5) illustrates the geographical boundaries of the agro-climatic regions used in subsequent drought analyses.

The Agricultural Drought Hazard Index (ADHI)

In the present study, a modified version of Adnan and Ullah's (2020) drought hazard assessment model was adopted to evaluate the severity of agricultural drought risk in Iran. This model integrates three principal components: **(a)** drought frequency—expressed as the proportion of drought years to the total period of record, **(b)** the dominant seasonal precipitation contribution index (S_Index), and **(C)** the ratio of dominant seasonal soil moisture to annual soil moisture ($\frac{SM_{i-j}}{SM_{Annual}}$). The formula is defined as follows:

$$DHI = \frac{1}{3}\left(\frac{T_d}{T_y} + S_{Index} + \frac{SM_{i-j}}{SM_{Annual}}\right) \quad (1)$$

Where:

- T_d: Total number of drought years,
- T_y: Total number of years in the study period,
- S_{Index}: index reflecting the agricultural system's dependence on the dominant seasonal rainfall at each station,
- SM_{i-j}: Soil moisture during the dominant precipitation season (e.g., July–September for monsoon, January–June for winter),
- SM_{Annual}: annual soil moisture.

Adnan and Ullah (2020) estimated S_Index by calculating the ratio of dominant seasonal rainfall to annual rainfall and assigning weights based on regional climatic context—primarily

dividing provinces into "Sindh" and "others" with relatively broad weighting categories (Table 3).

Unlike Pakistan, Iran is characterized by marked variations in seasonal precipitation regimes. Therefore, in this study, the dominant precipitation season at each station was first identified according to its highest contribution to annual precipitation. The range of the dominant season's percentage share was subsequently divided into four classes for each precipitation regime (winter, autumn, spring), with assigned weights from 1 to 4) according to the degree of reliance on that season. This weighting reflects regional variations in vulnerability by accounting for the criticality of the main rainfall season for agricultural activities.

The ADHI was then calculated for all stations using the above formula and categorized into five hazard classes, ranging from 'extremely high' to 'very low' (Table 4). This new structure allows the model to account for the diverse climate characteristics of Iran while enhancing its spatial reliability and interpretability compared to the original formulation by Adnan and Ullah (2020).

Table 3. Criteria used for the hazard assessment of drought using percentage of normal for rainfall for different regions of Pakistan.

Index	Class limit and rating score			
Percentage of Seasonal rainfall for Sindh province	>89	79 – 89	70 - 79	59 -60
Percentage of Seasonal rainfall for other provinces	>60	51 – 60	41 - 50	30 - 40
Index value	4	3	2	1

Reference: Adnan and Ullah (2020).

Table 4. Severity classes used in the ADHI map.

Hazard Classes	Hazard Index
Extremely High	> 1.50
High	1 - 1.50
Moderate	0.75 – 0.99
Low	0.60 – 0.74
Very low	< 0.60

Reference: Adnan and Ullah (2020).

Results and Discussion

patio-temporal Patterns of Soil Moisture

Analysis of the long-term monthly average soil moisture reveals pronounced spatio-temporal patterns that are fundamental to agricultural drought hazard in Iran (Fig. 3). Spatially, a stark dichotomy exists between the perennially humid northern Caspian coast, where moisture levels often exceed 400 mm/m, and the vast, chronically arid central, southern, and eastern regions, where values typically remain below 60 mm/m for most of the year. The western Zagros Mountains represent a transitional zone with moderately higher moisture content during the wet season. Temporally, a distinct annual cycle is evident nationwide. Soil moisture peaks in April, capitalizing on accumulated winter precipitation, and progressively declines to a

minimum in late summer (September-October) as evapotranspiration rates increase, leaving the majority of the country under severe moisture stress.

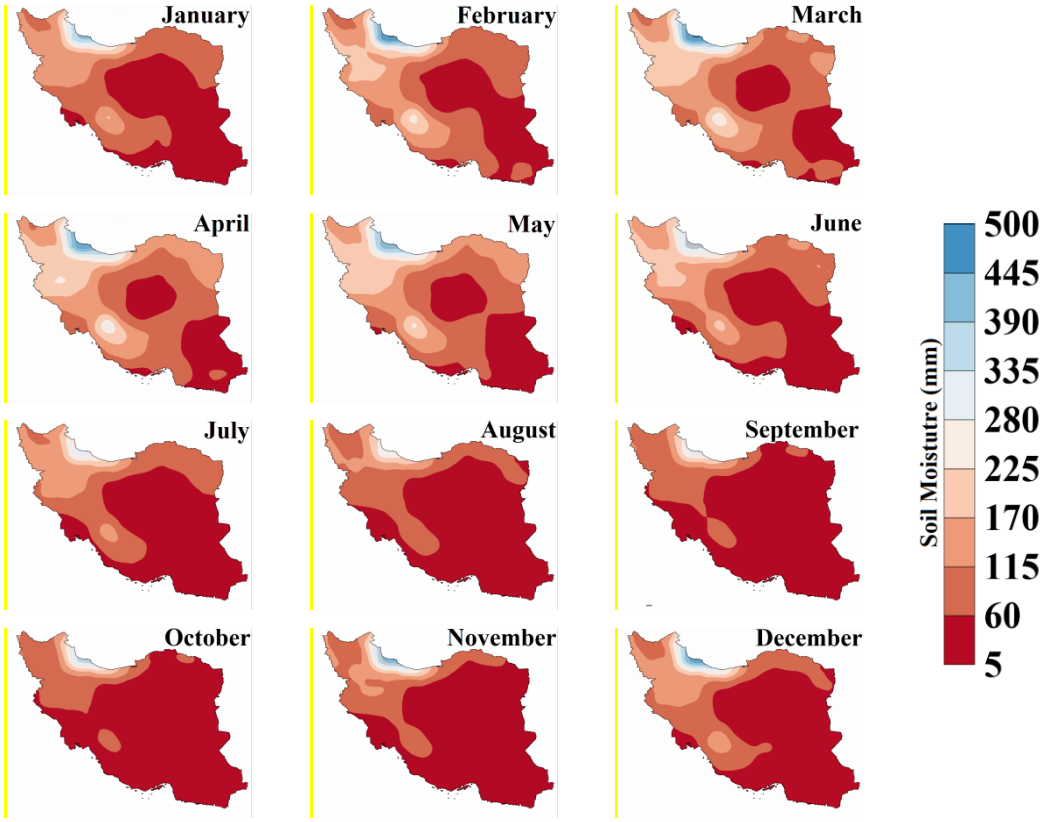

Figure 3. The spatial distribution of the monthly long-term average (1987-2016) of soil moisture in Iran based on the gridded data of soil moisture (Climate Prediction Center) (NOAA).

Spatio-temporal Distribution of Precipitation

Iran's precipitation climatology is defined by strong spatial gradients and pronounced seasonality (Fig. 4). Spatially, precipitation decreases markedly from the humid northern and western peripheries towards the arid central and eastern interior. This pattern is primarily controlled by orography; the Alborz and Zagros mountain ranges intercept moisture-bearing systems, leaving the vast central plateau in a rain shadow. Temporally, the climate is divided into a wet season (November-April) and a distinct dry season (May-October). During the wet season, the Caspian coast and Zagros highlands receive substantial rainfall, with January typically representing the peak precipitation month for much of the country. Conversely, from June to August, most of Iran, particularly the central and southern regions, experiences negligible rainfall. A notable exception is the Caspian region, which receives significant inter-seasonal rainfall, especially in early autumn.

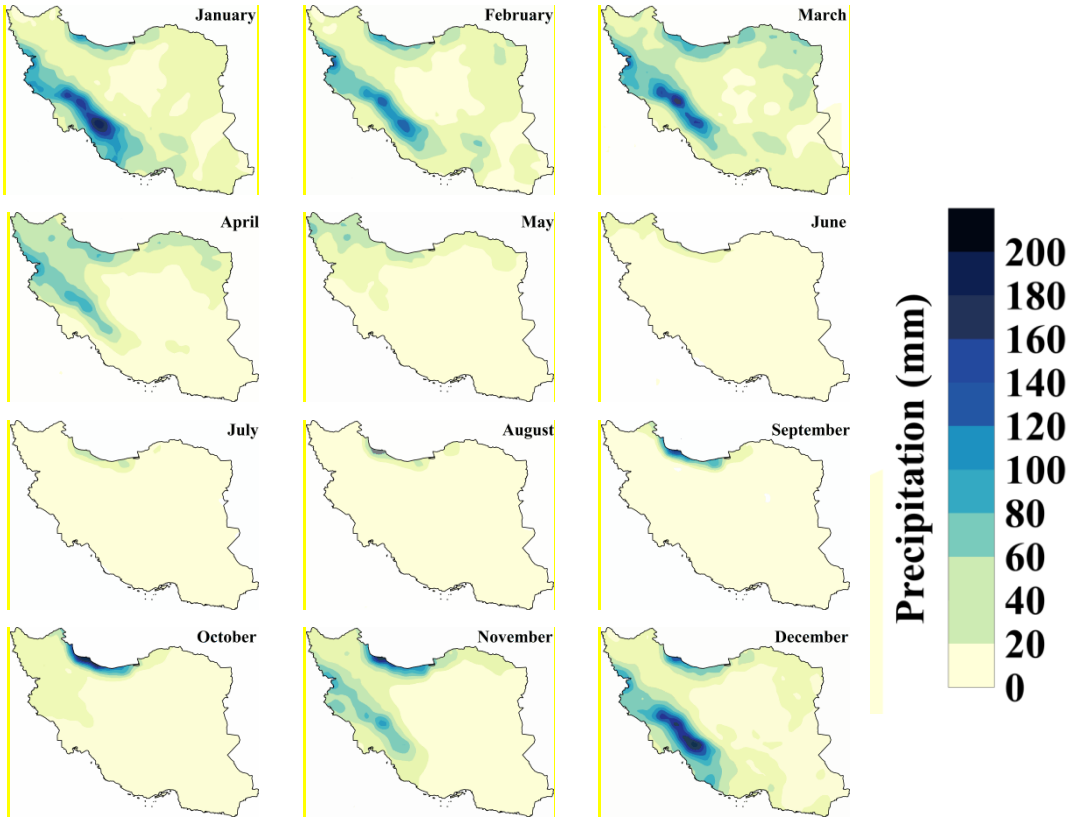

Figure 4. The spatial distribution of the monthly long-term average (1987-2016) of precipitation in Iran based on the data from 62 meteorological stations (1987-2016).

Coupling of Precipitation and Soil Moisture across Agro-Climatic Zones

The coupling strength between annual precipitation (SPI) and soil moisture (SSMI) was evaluated across Iran's distinct climatic zones (Fig. 5). The results, summarized in Table 5, reveal a distinct gradient where the correlation weakens from arid to humid environments. The coupling is exceptionally strong in Extremely Arid (r=0.70) and Arid zones, indicating that annual soil moisture is tightly controlled by precipitation anomalies. In contrast, the relationship becomes significantly weaker in Sub-Humid (r=0.22) and Very Humid (r=0.20) climates. This pattern suggests that in Iran's water-limited regions, the response of soil moisture to rainfall is direct and immediate. Conversely, in more humid zones, this linkage is buffered by moderating factors such as denser vegetation, higher soil water-holding capacity, and more complex hydrological processes, leading to a decoupled relationship.

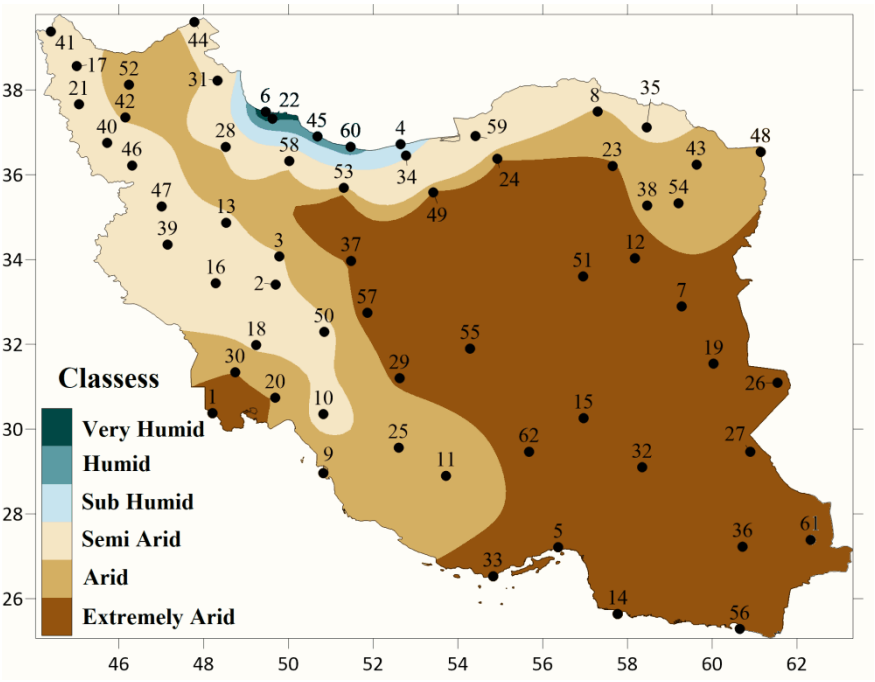

Figure 5. Iran's climatic classification based on the Moisture Index (MI). The numbers on the map are station codes assigned to each meteorological station (station names corresponding to each code are provided in Figure 2). This coding was applied to avoid overcrowding the map.

Table 5. Correlation analysis of the SPI and the SSMI for the six climatic classes of Iran.

Climate classification	Correlation between SPI and SSMI indices
Extremely arid	0.70
Arid	0.67
Semi-arid	0.55
Sub-humid	0.22
Humid	0.52
Very humid	0.20

The temporal evolution of meteorological (SPI) and agricultural (SSMI) drought from 1987–2016 is depicted in Figure 6 for each climatic zone. The analysis shows that agricultural drought years (SSMI<0) are a recurrent feature across all zones. The most persistent continuous agricultural drought was observed in the Arid region, lasting for eight consecutive years (2008–2015). Regarding drought severity, the most intense event (min SSMI ≈ -2.90) was paradoxically recorded in the Very Humid zone in 1999. A critical finding is the varying temporal alignment between the most severe meteorological (min SPI) and agricultural (min SSMI) droughts. In the Extremely Arid, Sub-Humid, and Very Humid zones, these peaks occurred concurrently, indicating a direct response. In contrast, a temporal lag was evident in the Arid, Semi-Arid, and Humid zones, where the most intense agricultural drought did not coincide with the year of the most severe precipitation deficit.

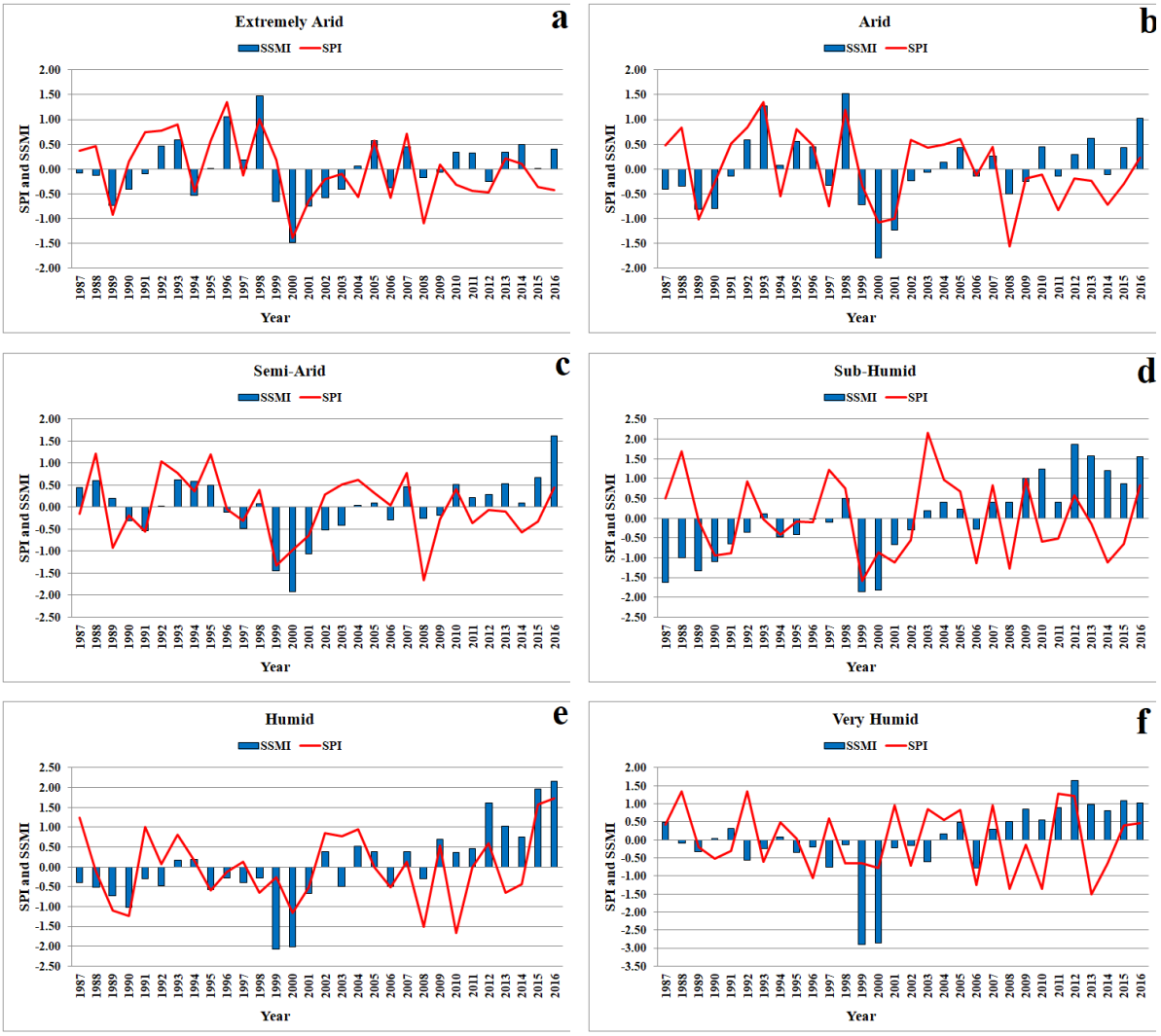

Figure 6. Time-series graphs of the SPI and the SSMI by each climatic class: a) extremely arid, b) arid, c) semi-arid, d) sub-humid, e) humid, and f) very humid, from 1987 to 2016.

The spatial pattern of the annual correlation between SPI and SSMI reveals a distinct climatic gradient across Iran (Figure 7). A strong positive correlation ($r>0.70$) dominates the arid and semi-arid southern and eastern regions, signifying that agricultural drought is a direct and immediate consequence of meteorological drought in these water-limited environments. In stark contrast, the correlation weakens significantly ($r<0.30$) in the humid northern and northwestern zones. This weaker relationship suggests that the link between precipitation deficits and soil moisture is more complex and buffered in these regions, likely modulated by factors such as different soil properties, denser vegetation, and the influence of snowmelt.

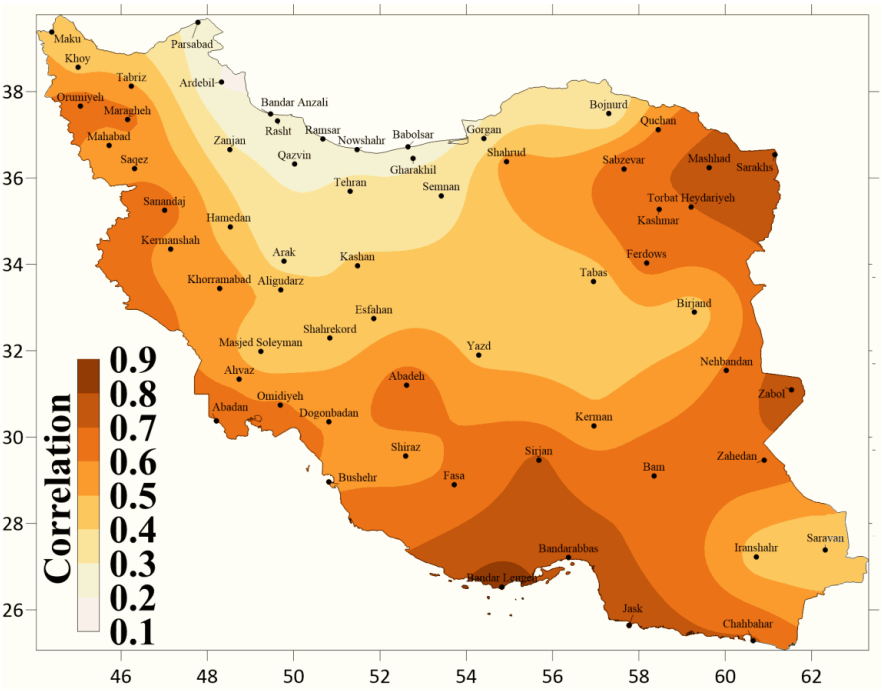

Figure 7. Spatial distribution of correlation between the SPI and the SSMI in Iran (from 1987 to 2016).

Spatio-temporal Distribution of Annual Meteorological Droughts (SPI) and Annual Agricultural Droughts (SSMI)

Figure 8 displays the annual spatial distribution of meteorological drought (SPI) from 1987 to 2016. A key observation is the pronounced inter-annual variability in the location and extent of drought, precluding a single, consistent spatial pattern. Despite this variability, the years 2008, 2000, and 1989 stand out as the most severe and widespread events, with drought conditions (SPI < 0) covering over 90% of Iran's territory.

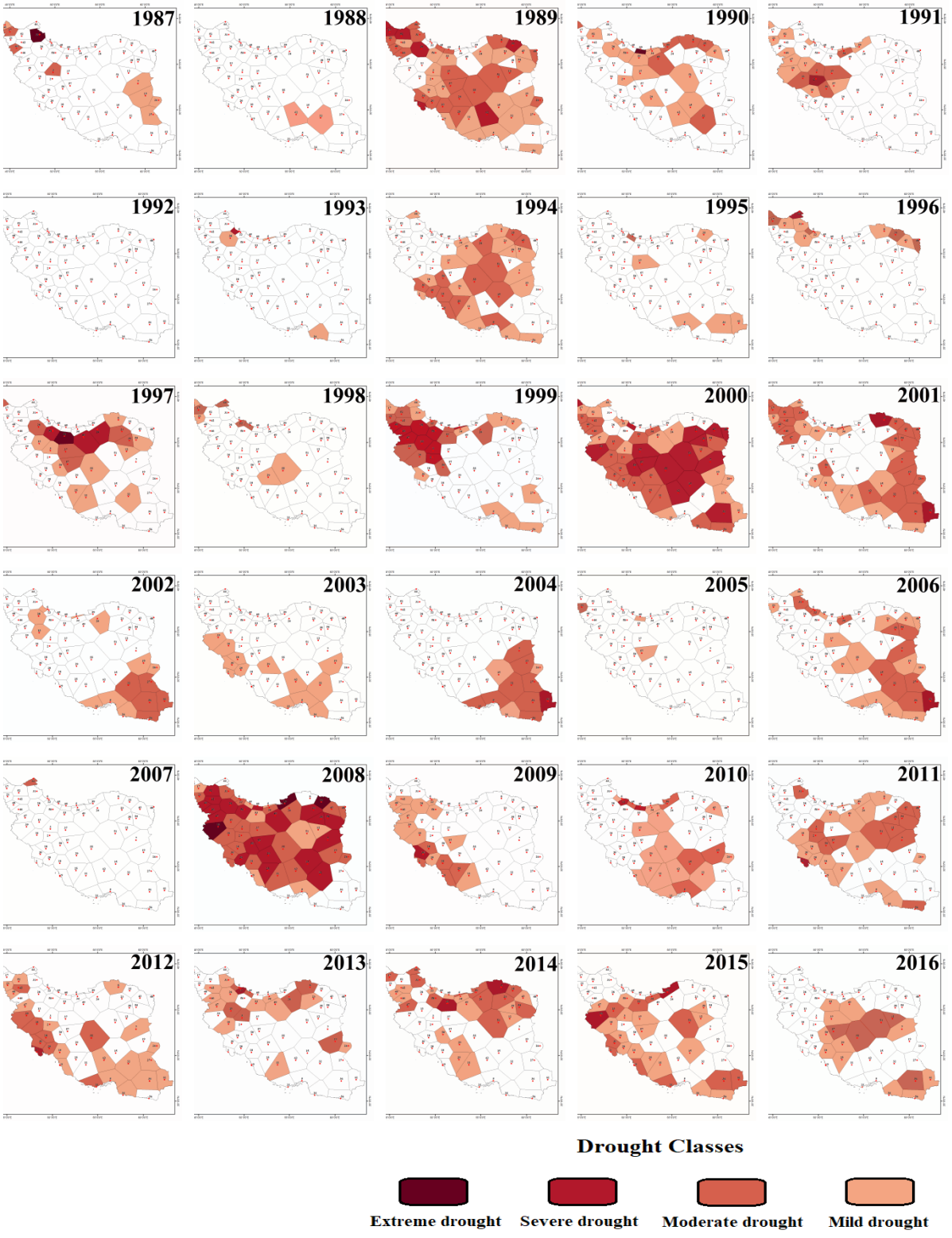

Figure 8. Spatial distribution of the various classes of meteorological droughts in Iran on an annual scale based on the SPI (from 1986 to 2015) using Thiessen's method.

Similarly, the spatial distribution of agricultural drought (SSMI) showed significant year-to-year variability in extent and severity (Figure 9). Analysis identifies 2000, 2001, 1999, and 1989 as the years with the most widespread and severe agricultural drought conditions.

336 Notably, the major drought years of 2000 and 1989 coincide with those identified by the SPI,
337 indicating periods where meteorological drought directly translated into extensive soil moisture
338 deficits across the country.

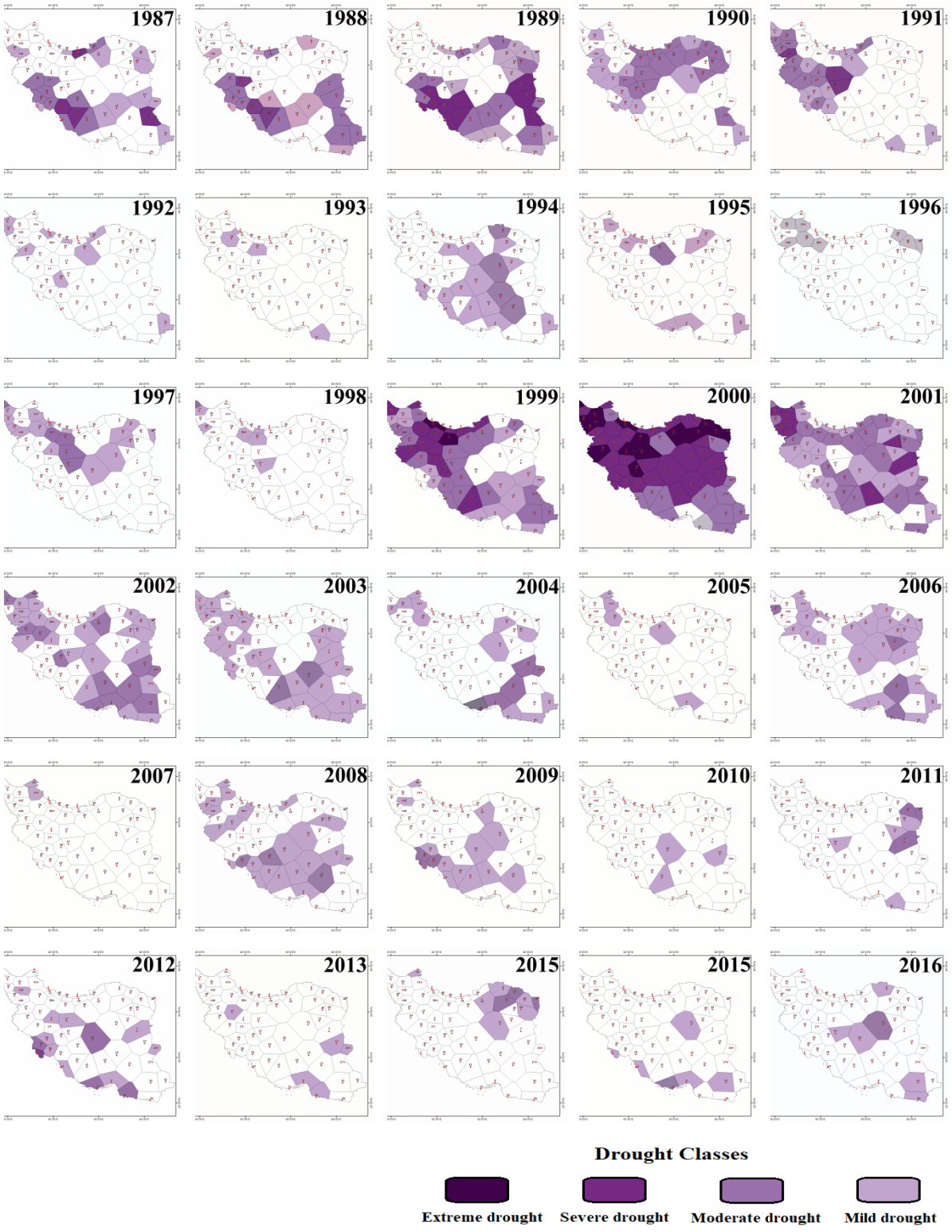

Figure 9. Spatial distribution of the various classes of agricultural droughts in Iran on an annual scale based on the SSMI (from 1986 to 2015) using Thiessen's method.

Frequency of Drought Severity Classes

Analysis of meteorological drought frequency (SPI) reveals a clear inverse relationship between severity and occurrence across Iran (Figure 10). Over the 30-year study period, mild and moderate droughts were by far the most prevalent classes. Conversely, the most intense events were rare; any given region experienced a maximum of approximately four severe droughts and only two extreme droughts.

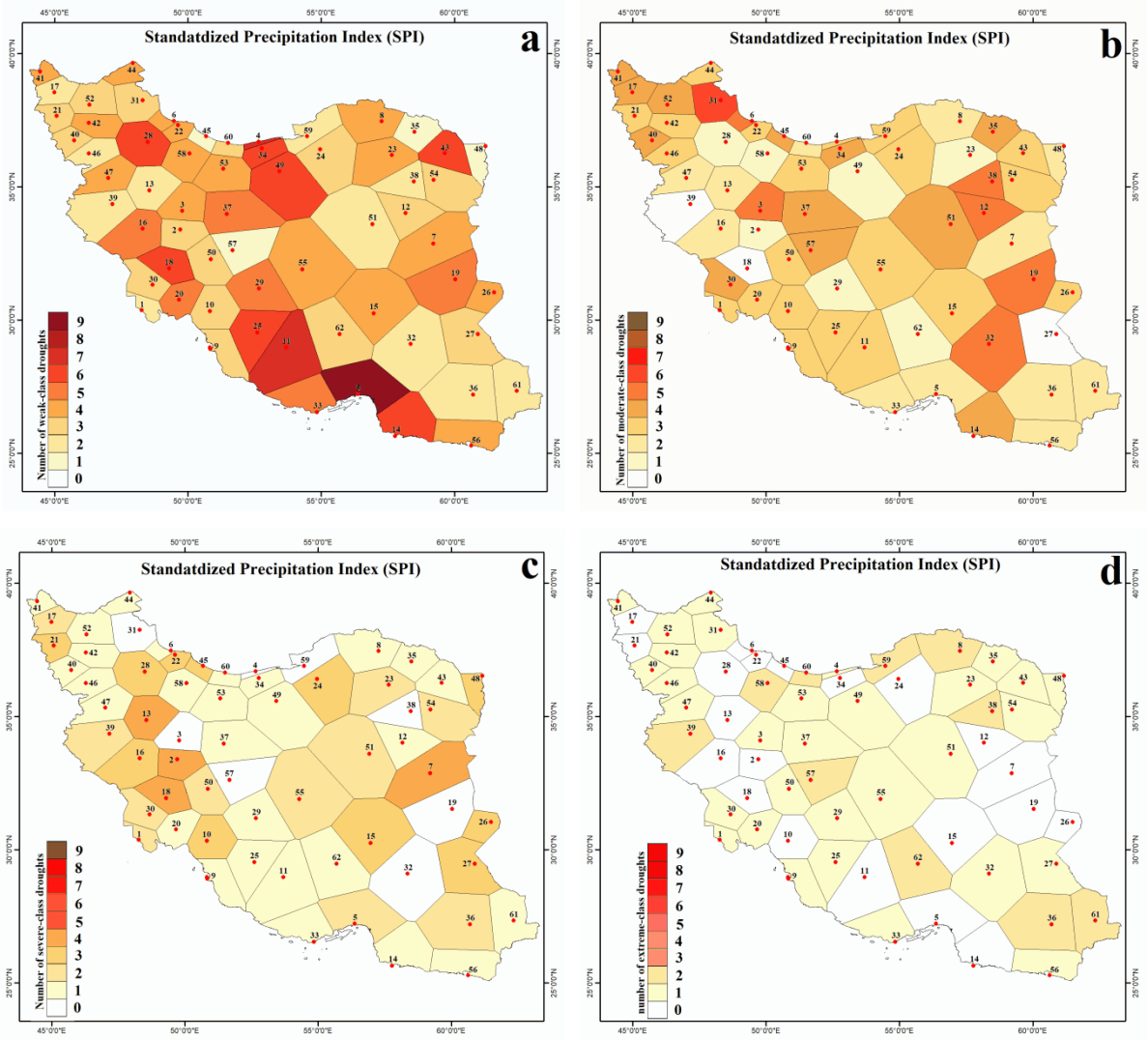

Figure 10. Spatial distribution of the various classes of droughts in Iran based on the SPI (1987-2016); a) the number of weak-class droughts; b) the number of moderate-class droughts; c) the number of severe-class droughts, and d) the number of extreme-class droughts over the course of 30 years.

The frequency of agricultural drought (SSMI) exhibits distinct spatial patterns that vary with severity (Figure 11). While weak droughts were widespread with no discernible large-scale pattern, a clear north-south divide emerged for more intense events. Moderate agricultural

droughts were significantly more frequent in the southern half of Iran, with some stations experiencing up to 7 occurrences. In a striking contrast, the highest frequencies of severe (up to 4 occurrences) and extreme (up to 2 occurrences) droughts were concentrated in the northern half of the country.

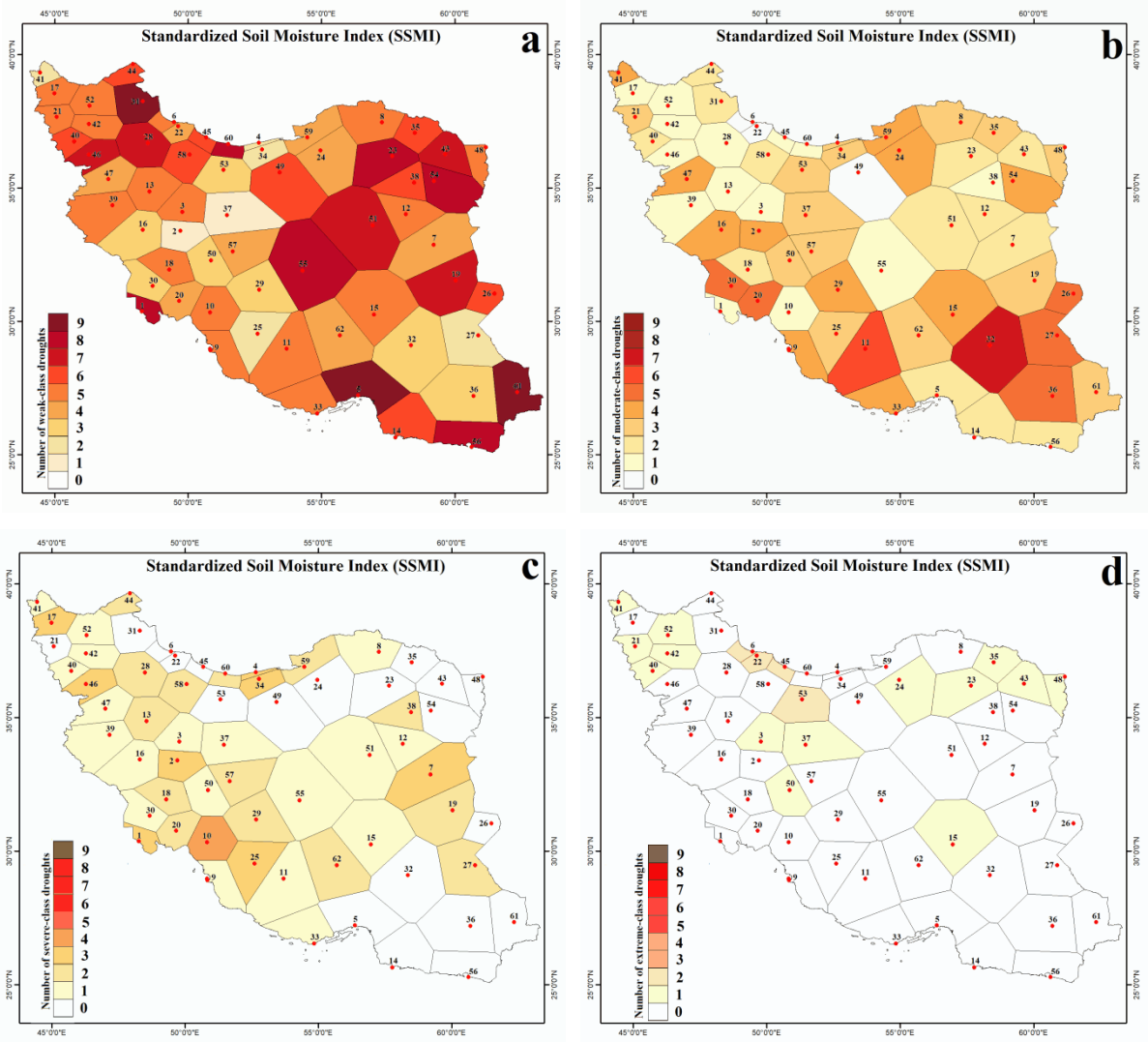

Figure 11. Spatial distribution map of the various classes of Iran's droughts using the SSMI for the 1987-2016 time period; a) the number of weak-class droughts, b) the number of moderate-class droughts, c) the number of severe-class droughts, and d) the number of extreme-class droughts over the course of 30 years.

Improving Iran's drought hazards index

To develop a map of Iran's drought hazards, this study utilized the Agricultural Drought Hazard Index (ADHI) proposed by Adnan and Ullah (2020). The calculation of the ADHI first requires determining the primary precipitation season for each station. This is achieved by calculating the ratio of precipitation received in each season (e.g., autumn, winter, spring, summer) to the total annual precipitation for each station. Subsequently, the season exhibiting the highest ratio of seasonal to total annual precipitation is identified as the dominant precipitation regime for

that station.

Figure 12 illustrates the spatial distribution of these dominant precipitation regimes across Iran based on data from 62 meteorological stations. According to this analysis, 50 stations are characterized by a winter precipitation regime. An autumn precipitation regime is dominant for 8 stations, primarily located in Iran's northern coastal areas along the southern boundaries of the Caspian Sea. A spring precipitation regime is observed at 4 stations, concentrated in the country's northwest. The remaining extensive areas of Iran predominantly experience a winter precipitation regime (Figure 12).

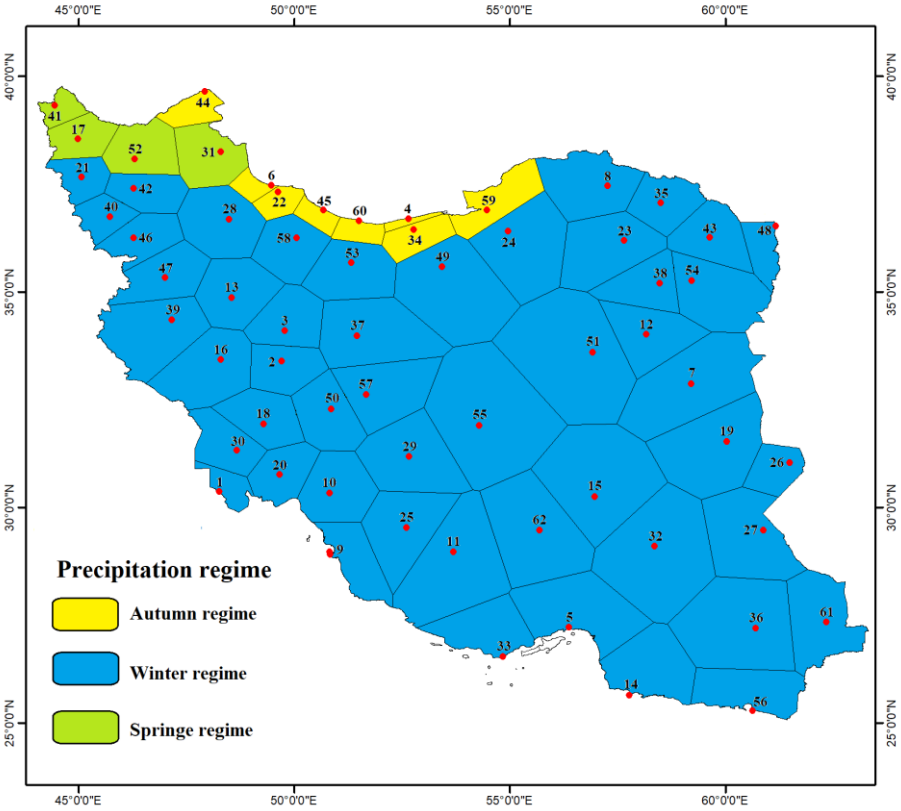

Figure 12. Precipitation regime (ratio of precipitation received in each season to the total annual precipitation) in Iran.

A region's heavy reliance on its primary rainy season can render it more vulnerable to drought if that season's precipitation fails (Adnan, 2015, 2016). To account for this, the precipitation regime of each station was weighted. For this purpose, we first identified the dominant precipitation season (winter, autumn, or spring) for groups of stations based on their geographical and climatological characteristics (as previously described for Figure 12). Then, for all stations within each identified regime, we determined the lowest and highest ratios of that dominant season's precipitation to the total annual precipitation.

- For stations within the winter precipitation regime, seasonal contributions ranged from 32% to 71% of the annual total.
- For stations within the autumn precipitation regime, seasonal contributions ranged from 30% to 49% of the annual total.
- For stations within the spring precipitation regime, seasonal contributions ranged from 31% to 46% of the annual total.

Each of these numerical ranges (min to max seasonal contribution for a given regime) was then divided into four approximately equal intervals (classes). Each class was assigned a weight from 1 (representing stations where the dominant season contributes a smaller fraction to the annual total, thus indicating relatively less vulnerability to that specific season's failure) to 4 (representing stations where the dominant season contributes a larger fraction, indicating higher vulnerability). The specific class ranges and assigned weights for each regime are detailed in Table 6. For instance, within the winter precipitation regime (overall range 32-71%), stations with seasonal contribution ratios of 32-41% received a weight of 1, 42-51% a weight of 2, 52-61% a weight of 3, and 62-71% a weight of 4. A similar procedure of dividing the regime-specific range into four classes was applied to derive the weights for the autumn and spring precipitation regimes.

The main methodological distinction of this study from that of Adnan and Ullah (2020) lies in the classification of precipitation regimes. Adnan and Ullah (2020), in their ADHI calculation for Pakistan, divided precipitation regimes into two broad categories: seasonal precipitation of Sindh province and seasonal precipitation of other provinces (refer to their Table 3). Such a division is not readily generalizable to other regions of the world with different climatic characteristics. Therefore, this study aimed to adapt their approach by introducing a new classification that encompasses the different types of precipitation regimes found in Iran and their respective numerical contributions (Table 6).

After determining the precipitation regime for each station (as shown previously in Figure 12) and assigning the corresponding weights (Table 6), the Agricultural Drought Hazard Index (ADHI) for each station was calculated. The ADHI calculation also required data on all weak, moderate, and severe droughts that occurred during the study period at each station on an annual scale (identified from SPI analysis), as well as the seasonal and annual soil moisture values at each station (extracted from CPC gridded data, specific to each station's precipitation regime). Finally, using Equation 1 (detailed in the Data and Methodology section), the ADHI for all 62 stations in Iran was computed. The results of this index were classified into five

categories: 'extremely high', 'high', 'moderate', 'low', and 'very low', following the classification scheme presented in Table 4 (which has been previously used by Asrari et al., 2012 and Adnan and Ullah, 2020).

Table 6 Weighting criteria for Iran's precipitation regimes based on the percentage contribution of the dominant season to total annual precipitation, used in ADHI calculation.

Precipitation regime	The range of classes and the weight assigned to each class			
autumn	30-34	35-39	40-44	**45-49**
winter	32-41	42-51	52-61	**62-71**
spring	31-34	35-38	39-42	**43-46**
assigned weight	1	2	3	**4**

The map of Iran's Drought Hazard Index is presented in Figure 13. According to this map, most areas of Iran are vulnerable to drought. However, the central, southern, and southeastern regions of Iran exhibit higher vulnerability compared to other regions. Out of the 62 studied stations, 9 stations were found to have an 'extremely high' drought hazard, 20 stations were 'high', 22 stations were 'moderate', 0 stations were 'low', and 11 stations were classified with 'very low' drought hazard (Figure 13).

According to Iran's administrative divisions, the provinces of Sistan and Baluchestan, Kerman, South Khorasan, Hormozgan, Yazd, Razavi Khorasan, and Fars are the most vulnerable provinces in the country. All these provinces are located in the central, southern, southeastern, and eastern parts of Iran and are characterized by arid climates. Notably, the two provinces of Mazandaran and Gilan, located on the southern coasts of the Caspian Sea (northern Iran), which have humid climates, are also identified among the provinces with high vulnerability to drought according to this index. The reason for the vulnerability of these provinces, especially the southern ones, to drought is their heavy reliance on seasonal precipitation, as most of their significant rainfall occurs only in winter. Therefore, a deficit in this seasonal precipitation has led to severe droughts in these provinces. Meanwhile, provinces located in the northwest, west, and northeast demonstrate the lowest vulnerability to drought, which is attributed to the distribution of their annual precipitation over two or three seasons.

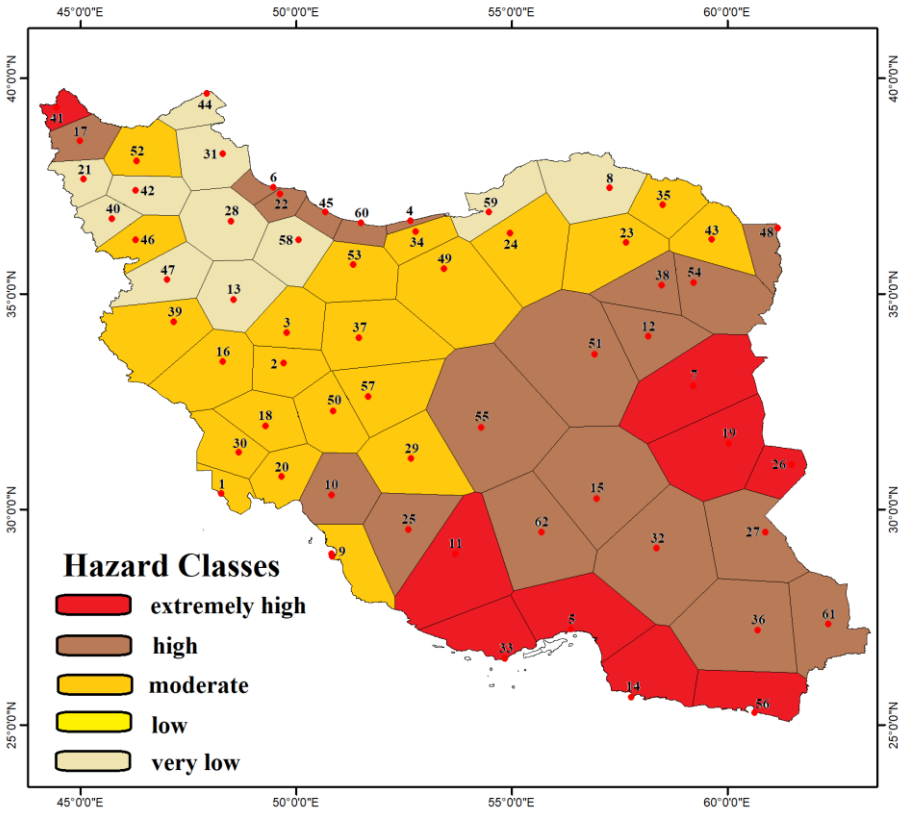

Figure 13. Iran's Agricultural Drought Hazard Index (ADHI) map.

Conclusions

This study successfully developed the first comprehensive, national-scale Agricultural Drought Hazard (ADH) map for Iran by synthesizing standardized indices for precipitation (SPI) and soil moisture (SSMI). The analysis identifies a critical vulnerability corridor spanning the central, southern, and southeastern regions, classifying them under high to extreme drought hazard. The primary contribution of this work lies in its integrated methodology; by correlating and combining meteorological drivers with agricultural impacts (soil moisture deficits) across Iran's diverse climatic zones, the study moves beyond single-indicator assessments to provide a more robust and holistic hazard evaluation. This spatially explicit ADH map serves as an essential evidence-based tool for policymakers, enabling the prioritization of resources and the development of targeted adaptation strategies to enhance agricultural resilience in the nation's most vulnerable areas. Future research should focus on refining this framework by incorporating dynamic vulnerability indicators and higher-resolution remote sensing data to further improve drought early warning systems.

References

1. Achite, M., O. Bazrafshan, O. M. Katipoğl, Z. Azhdari. 2023. "Evaluation of hydro-meteorological drought indices for characterizing historical droughts in the Mediterranean climate of Algeria." *Nat. Hazards.* 118: 427–453.
2. Adnan, S., K. Ullah. 2020. "Development of drought hazard index for vulnerability assessment in Pakistan." *Nat. Hazards.* 103: 2989–3010.
3. Adnan, S., K. Ullah, S. GAO. 2015. "Characterization of drought and its assessment over Sindh, Pakistan during 1951–2010." *J. Meteorol. Res.* 29: 837–857.
4. Asakereh, H. 2011. Fundamentals of Statistical Climatology. [In Persian.] Zanjan University press, Zanjan, Iran.
5. Asrari, E., M. Masoudi, S. S. Hakimi. 2012. "GIS overlay analysis for hazard assessment of drought in Iran using Standardized Precipitation Index (SPI)." *J. Ecol. Environ.* 35: 323–329.
6. Avia, L. Q., E. Yulihastin, M. H. Izzaturrahim, R. Muharsyah, H. Satyawardhana, I. Sofiati, E. Nurfindarti, S. Gammamerdianti. 2023. "The spatial distribution of a comprehensive drought risk index in Java, Indonesia." *Kuwait J. Sci.* 50(4): 753-760.
7. Berhail, S., O. M. Katipoğlu. 2023. "Comparison of the SPI and SPEI as drought assessment tools in a semi-arid region: case of the Wadi Mekerra basin (northwest of Algeria)." *Theor. Appl. Climatol.* 154: 1373-1393.
8. Bettahar, A, Ş. Şener. 2022. "Analysis of meteorological drought indices in the Wadi Righ area (southern Algeria)." *Sustain. Water Resour. Manag.* 8: 152.
9. Blauhut, V., L. Gudmundsson, K. Stahl. 2015. "Towards pan-European drought risk maps: quantifying the link between drought indices and reported drought impacts." *Environ. Res. Lett.* 10: 14008.
10. Byun, H. R., D. A. Wilhite. (1999). "Objective quantification of drought severity and duration." *J. Clim.* 12: 2747–2756.
11. Cao, S., Y. He, L. Zhang, Y. Chen, W. Yang, S. Yao, Q. Sun. 2021. "Spatio-temporal characteristics of drought and its impact on vegetation in the vegetation region of Northwest China." *Ecol. Indic.* 133: 108420.
12. Chanda, K., R. Maity, A. Sharma, R. Mehrotra. 2014. Spatio-temporal variation of long-term drought propensity through reliability-resilience-vulnerability based drought management index. *Water. Resour. Res.* 50: 7662–7676.

13. Daneshvar, M. R. M., A. Bagherzadeh, M. Khosravi. 2012. "Assessment of drought hazard impact on wheat cultivation using standardized precipitation index in Iran." *Arab. J. Geosci.* 6: 4463–4473.
14. Das, P. K., R. Das, D. K. Das, S. K. Midya, S. Bandyopadhyay, U. Raj. 2020. "Quantification of Agricultural Drought over Indian Region: A Multivariate Phenology-Based Approach." *Nat. Hazards*, 101: 225–274.
15. De Martonne, M. 1909. "Traité de géographie physique – Climat – Hydrographic – Relief du sol – Biogéographie." Paris : Li-brairie Armand Colin..
16. Erfurt, M., R. Glaser, V. Blauhut. 2019. "Changing impacts and societal responses to drought in southwestern Germany since 1800." *Reg. Environ. Change,* 19: 2311–2323.
17. Fan, Y. and H. van den Dool. 2004. "Climate prediction center global monthly soil moisture data set at 0.5 degree resolution for 1948 to present." *J. Geophys. Res.* 109(10): D10102.
18. Faridatul, M. I., B. Ahmed. 2020. "Assessing Agricultural Vulnerability to Drought in a Heterogeneous Environment: A Remote Sensing-Based Approach." *Remote. Sens.* 12(20): 3363.
19. Free worlds maps. 2021. Iran Physical map. https://www.freeworldmaps.net/asia/iran/map.html
20. Gautam, S., A. Samantaray, M. Babbar-Sebens, M. Ramadas. 2023. "Characterization and Propagation of Historical and Projected Droughts in the Umatilla River Basin, Oregon, USA." *Adv. Atmos. Sci.* 41: 247-262.
21. Ghorbani, H., A. A. Vali, H. Zarepour. 2019. Analysis of the Climatological Drought Trend Variations Using Mann-Kendall, Sen and Pettitt Tests in Isfahan Province. [In Persian.] Journal of Spatial Analysis Environmental Hazards, 6 (2), 129-146.
22. Hagenlocher, M., I. Meza, C. C. Anderson, A. Min, F. G. Renaud, Y. Walz, S. Siebert, Z. Sebesvari. 2019. "Drought vulnerability and risk assessments: state of the art, persistent gaps, and research agenda." Environ. Res. Lett 14: 083002.
23. Kao, S. C., R. S. Govindaraj. 2010. "A copula-based joint deficit index for droughts." *J. Hydrol.* 380(1–2): 121–134.
24. Katiraie-Boroujerdy, P. S., N. Nasrollahi, K. L. Hsu, S. Sorooshian. 2013. "Evaluation of satellite-based precipitation estimation over Iran." *J. Arid Environ.* 97: 205-219.

25. Kim, H., J. Park, J. Yoo, T-W. Kim. 2015. "Assessment of drought hazard, vulnerability, and risk: a case study for administrative districts in South Korea." *J. Hydro-environment. Res.* 9(1): 28–35.
26. Lin, W., C. Wen, Z. Wen, H. Gang. 2015. "Drought in Southwest China: A review." *Atmos. Ocean. Sci. Lett.* 8: 339–344.
27. Mahmoudi, P., A. Rigi, M. Miri Kamak. 2019a. "A comparative study of precipitation-based drought indices with the aim of selecting the best index for drought monitoring in Iran." *Theor. Appl. Climatol.* 137: 3123–3138.
28. Mahmoudi, P., M. Hamidian Pour, M. Sanaei, N. Daneshmand. 2019b. "Investigating the Trends of Drought Severity Changes in Iran. In: Proceedings of International Conference on Climate Change, Impacts, Adaptation and Mitigation, 11 June, Kharzmi University, Tehran, Iran.
29. Mahmoudi, P., R. Maity, S. M. Amir Jahanshahi, K. Chanda. 2022. "Changing spectral patterns of long-term drought propensity in Iran through reliability–resilience–vulnerability-based Drought Management Index." *Int. J. Climatol.* 42(8): 4147–4163.
30. McKee, T. B., N. J. Doesken, J. Kleist. 1993. "The Relationship of Drought Frequency and Duration to Time Scales." Proceedings of the 8th Conference on Applied Climatology, 17–22 January 1993, Anaheim, CA. Boston, MA.
31. Modarres, R. 2007. "Streamflow drought time series forecasting." *Stochastic Environ. Res. Risk Assess.* 21(3): 223–233.
32. Nasrollahi, M., H. Khosravi, A. Moghaddamnia, A. Malekian, S. shahid. 2018. "Assessment of drought risk index using drought hazard and vulnerability indices." *Arab. J. Geosci.* 11: 606.
33. Natarajan, N., M. Vasudevan, S. A. Raja, K. Mohanpradaap, G. Sneha, S. J. Shanu. 2023. "assessment methodology for drought severity and vulnerability using precipitation-based indices for the arid, semi-arid and humid districts of Tamil Nadu, India." *Water Supply*, 23(1): 54-79.
34. Palmer, W .C. 1965. "Meteorological Drought." Research Paper No. 45. US Department of Commerce Weather Bureau, Washington D C, pp. 1-58.
35. Shahid, S., H. Behrawan. 2008. Drought risk assessment in the western part of Bangladesh. *Nat. Hazards,* 46(3):391–413.
36. Thiessen, A. H. 1911. "Precipitation averages for large areas." *Mon Weather Rev*. 39: 1082–1084.

37. Vaghefi, S. A., M. Keykhai, F. Jahanbakhshi, J. Sheikholeslami, A. Ahmadi, H. Yong, K. C. Abbaspour. 2019. "The future of extreme climate in Iran." *Sci. Rep.* 9: 1-11.
38. van den Dool, H., J. Huang, Y. Fan. 2003. "Performance and analysis of the constructed analogue method applied to US soil moisture applied over 1981–2001." *J. Geophys. Res.* 108: 1–16.
39. Vicente-Serrano, S., S. Beguería, J. L. López-Moreno. 2010. "A multiscalar drought index sensitive to global warming: the standardized precipitation evapotranspiration index." *J. Clim.* 23(7): 1696-1718.
40. Wilhite, D. A. 2005. "Drought." In: Oliver, J.E. (eds) Encyclopedia of World Climatology. Encyclopedia of Earth Sciences Series. Springer, Dordrecht.
41. Yu, J., J. Lim, K. S. Lee. 2018. Investigation of drought-vulnerable regions in North Korea using remote sensing and cloud computing climate data. *Environ. Monit. Assess.* 190: 126.